Effect of Peer Influence and Looting Concerns on Evacuation Behavior During Natural Disasters

Matthew Hancock¹, Nafisa Halim², Chris J. Kuhlman¹ and Achla Marathe¹, Pallab Mozumder³, S. S. Ravi¹, and Anil Vullikanti¹

¹ University of Virginia, Charlottesville VA 22904, USA, mgh3x@virginia.edu,hugo3751@gmail.com,achla@virginia.edu, ssravi0@gmail.com,vaskumar@virginia.edu,
² Boston University, Boston MA 02218, USA, nhalim@bu.edu,
³ Florida International University, Miami FL 33199, USA, mozumder@fiu.edu

Abstract. We study evacuation dynamics in a major urban region (Mi-ami, FL) using a combination of a realistic population and social contact network, and an agent-based model of evacuation behavior that takes into account peer influence and concerns of looting. These factors have been shown to be important in prior work, and have been modeled as a threshold-based network dynamical systems model (2mode-threshold), which involves two threshold parameters—for a family's decision to evacuate and to remain in place for looting and crime concerns—based on the fraction of neighbors who have evacuated. The dynamics of such models are not well understood, and we observe that the threshold parameters have a significant impact on the evacuation dynamics. We also observe counter-intuitive effects of increasing the evacuation threshold on the evacuated fraction in some regimes of the model parameter space, which suggests that the details of realistic networks matter in designing policies.

Keywords: network science, graph dynamical systems, agent-based models, natural disasters, evacuation

1 Introduction

Background and Motivation. The 2020 Atlantic hurricane season produced 30 named storms, of which 14 developed into hurricanes, and 7 intensified into major hurricanes. It was the most active season on record and the fifth consecutive above-average season since 2016. Total estimated costs to the U.S. from hurricanes and tropical storms in 2020 was \$95 billion, which was the 4th largest inflation-adjusted annual cost and more than twice the 41 year average of \$45.7 billion since 1980 [16]. See [13] for more details about hurricane season 2020 and others. Over the years, hurricanes are becoming more frequent and more intense, and inflict major physical and economic damage annually [15].

Timely evacuation during a hurricane can lead to greater safety and may even save lives. Not heeding evacuation orders can not only put individuals' lives at risk but also the lives of first responders. Power outage, flooding, issues with water supply, access to internet, food, etc. can make it hard to survive without help from emergency workers. However, there are many factors that go into a family's decision of whether or not to evacuate in the face of an oncoming hurricane. These can be broken into categories such as storm characteristics, family demographics, geography, and risk perceptions. Two factors that are of particular importance are: (i) evacuation behavior of peers, which can influence others to evacuate and (ii) concerns about looting and crime, if too many people evacuate from the neighborhood. Looting has a countering effect to peer influence on evacuation: concerns over looting in a depopulated area may inhibit families from leaving who would otherwise evacuate [9].

Our Contributions. We study the impact of peer influence and looting on evacuation during a natural disaster, using a detailed agent-based simulation (ABS) of a network dynamical system model. While the underlying network is realistic, the dynamical system model is stylized, and our goal is to understand its phase space properties. In another paper submitted to this conference, we study how survey data can be combined with agent based models; the analysis in this paper can help in validation of such methods. This paper takes a more mechanistic approach to evacuation modeling; the other paper takes a more data-driven approach. The former approach has the benefit that mechanistic models are typically more transferable to other situations (e.g., different hurricanes in different cities); the latter has the benefit that the model is guided by real data. Our ultimate goal is to combine these two approaches, but each is significant in its own right. Our specific contributions in this work are summarized below.

- 1. Study of evacuation behavior in a large urban region using detailed agent-based models. We develop a detailed agent-based model (ABM) for evacuation in Miami, FL. This combines a high resolution population and social contact network of Miami, with an ABM of evacuation. The population model integrates diverse kinds of commercial and open source datasets, including U. S. Census, American Community Survey (ACS), Public Use Microdata Sample (PUMS), National Household Travel Survey (NHTS), transportation network data, and land use data (see a summary of this process in [2,5]). Our agent-based evacuation behavior model represents peer influence and concerns of looting, as in [9], but considers more realistic parameter ranges.
- 2. Simulation based analysis of evacuation behavior. First, we provide some terminology; these concepts are detailed in Section 3. The evacuation threshold η_{min} (respectively, the looting threshold $(\eta_{min} + \eta_c)$) is the minimum (respectively, maximum) fraction of neighbors of a non-evacuating family (node) v_i in the social network G that must be in the evacuating stating for v_i to have a non-zero probability of evacuating. Hence, η_c is the regime over the range [0, 1] in fraction of neighbors evacuating where a family has a non-zero probability of evacuation.

We present several new findings. First, in past work [9], the evacuation threshold η_{min} was taken as a fixed value, slightly greater than zero (value 0.0001), which fostered spread of contagion. In this work we systematically study the ef-

fect of η_{min} , and demonstrate a somewhat counterintuitive result: for a fixed η_c , the fraction of evacuating families can increase as η_{min} increases, if the non-zero probability of evacuation $p_{e,max}$ is sufficiently large. Other findings include, a precipitous drop in the fraction of evacuating families for increases in η_{min} over a narrow range, suggestive of a phase transformation. This phenomenon is robust across numbers of seed nodes and probabilities of evacuation $p_{e,max}$. Finally, the effect of η_c can be large or small; it is largest for lesser $p_{e,max}$ and lesser η_{min} . But noteworthy is that the effect of η_c captures the primary difference between the looting model and a standard threshold model (see Section 3 for details), because as $\eta_c \to (1 - \eta_{min})$, the looting model transforms to the standard relative threshold model. We find that for conditions studied in this work, evacuation rates saturate and the peak fraction of evacuations on any given day saturates at much lesser values of η_c , i.e., saturation of the looting model behavior to the behavior of the standard relative threshold model occurs for $\eta_c \ll (1 - \eta_{min})$.

3. Spatial extent of evacuating families. The population model provides detailed spatio-temporal information for all individuals. We zoom in on the highest household density region of Miami to evaluate spatial differences in evacuation rates. We grid this region in to roughly 20,000 rectangular cells and compute the average evacuation rate of all families within each cell, and plot these results as heatmaps. Quite surprisingly, we find that although there are variations, the average evacuation rates are largely homogeneous in space.

Novelty of Our Work. Our work is the first to study the role of peer influence and looting behavior on a high resolution synthetic population in a major urban region. While the specific dynamical system model we use here was proposed in prior work [9], their analysis was restricted to a smaller region (Virginia Beach, VA), and used a stylized Kleinberg small-world network, instead of more realistic contact structure based on diverse transportation and land use datasets, as we do here. We find that the realistic network structure does have an impact on the observed evacuation behavior. We also find the model is quite sensitive to the parameters, which was not studied before. Our work points to the importance of representing realistic populations in such analyses. Other (urban) populations can be studied.

Related Work. We divide related work into the following two themes.

Factors influencing evacuation decisions. Factors important to families in evacuation decision-making are: receiving an evacuation notice, traffic gridlock, presence of children and pets, age of decision-makers, the household's education level, property protection, household income, work duties, race, availability of resources, and having somewhere to stay [12,14,17]. According to [3,6], the most important factors in choosing to evacuate are past evacuation experience, effective communication of the risks of staying, and social influences such as support networks and watching peers evacuate. The most important factors in choosing not to evacuate are territoriality, wanting to protect from looters, underestimating the severity of the hurricane, and overestimating household safety [14]. Extensive media reporting of looting and rioting during Hurricane Katrina caused officials to strongly warn against it in subsequent natural disasters [7].

4 Matthew Hancock et al.

Evacuation models and simulations. In [18], an ABM models hurricane evacuation in the Miami-Dade area for a hypothetical category-4 hurricane. Focus is placed on shadow evacuation, or evacuation occurring outside of the mandatory evacuation zone. An ABM based on survey data models Hurricane Sandy in northern New Jersey [19]. In [12], an evacuation model was developed from survey data from persons' experiences of Hurricane Sandy. This model includes factors of peer influence, looting, and household demographics. The work closest to our is [9]; our extensions of that work are covered in the novelty section.

2 Family Social Contact Network

We briefly summarize the realistic population and social contact network model for Miami, FL, which we use in our paper; we refer to [2,5] for complete details about this model. Each individual in the population is represented. Individuals are organized into households, which are geolocated. A census of these households at a block group level is statistically indistinguishable from the U.S. census. Each individual has a normative daily activity schedule, e.g., work, school, home, and shopping activities etc., with each activity being assigned a location and a start and an end time. Two people who visit the same location, with overlapping times of visit, are assumed to come into contact with each other.

In this way, an individual-based social contact network is generated: each individual is a node in the network, and an undirected edge is placed between two nodes if they visit the same location and their visits overlap in time. In our context, contact between individuals implies communication between individuals about evacuation and an opportunity to influence each other. For evacuation related decision-making purposes, we assume that only those people in the age range 18 to 70, inclusive, are relevant and hence only consider edges in the network between such persons. Younger (and older) individuals that might have additional information from sources like social media are not taken into account.

Table 1: Structural properties of a family-based social contact network of Miami, FL. Nodes are families and edges are interactions between families. Properties computed with the cyberinfrastructure net.science [1].

Network	Num.	Num.	Edges	Avg.	De-	Max.	De-	Avg.	Diameter
	Nodes			gree		gree		Clust.	
								Coeff.	
Miami, FL	1,702,038	42,789,	880	50.3		760		0.045	9

Since evacuation decisions are made at the family level, we construct a family social contact network from the individual-based network. In this network, nodes are now families. Two families interact (communicate, form an undirected edge) if there is at least one edge between one person in one family and one person in the second family in the individual-based social network, and both are between 18 and 70 years old. This network has 1.70 million nodes (families) and 42.8 million edges; see Table 1 for selected structural properties. Data used to generate the individuals, the demographics (e.g., age, gender), family compositions, and activity patterns and locations include, but not limited to,

American Community Survey (ACS), Public Use Microdata Sample (PUMS), National Household Travel Survey (NHTS), HERE (here.com), National Center for Education Statistics (NCES), U. S. Census data, Dun and BradStreet, and Open Street Maps. See [2,5] for details.

3 Models

3.1 Network Model

The family social contact network (FSCN) is the graph G(V, E), with node set V and edge set E, where each family $v_i \in V$, $i \in \{1, 2, ..., n\}$ is a node in the graph and n = |V|. An undirected edge is placed between two nodes v_i and v_j to form edge $e_{ij} = \{v_i, v_j\}$, $e_{ij} \in E$ (i.e., v_i and v_j communicate) if and only if at least one family member of v_i is co-located with at least one family member of v_i , and both family members are in the age group 18-70.

3.2 Peer Influence Contagion Models

Figure 1 contains the two models used in this study to quantify a family's decision-making process in determining whether it will evacuate in the face of an on-coming hurricane, on any particular day. The models are general so that each family v_i can have different properties such as threshold $\eta_{min,i}$ and maximum daily probability of evacuation $p_e = p_{e,max,i}$. However, for this paper, we use homogeneous properties so that $\eta_{min,i} = \eta_{min}$ and $p_{e,max,i} = p_{e,max}$, etc., for all $i \in \{1, 2, ..., n\}$.

In both models, a node at each time t has a state in $K = \{0, 1\}$. For node v_i , state $s_i = 0$ means that v_i is not evacuating; state $s_i = 1$ means that v_i is evacuating. For each v_i , there is a function $f_i : K^{d(v_i)} \to K$ that defines the process by which a node changes state from $s_i = 0$ to $s_i = 1$. Once a node reaches state 1, it stays in state 1, which is a progressive threshold model [10]. The two models differ in the forms of f_i .

The first model is the standard-threshold model in Figure 1a, and is based on the relative threshold model in [4]. Each node v_i has an evacuation threshold $\eta_{min} \in [0.0, 1.0]$ and denotes the minimum fraction of its neighbors that must be in state 1 (i.e., evacuating) in order for v_i to change state from $0 \to 1$. Let η_1 be the fraction of neighbors of v_i that are in state 1. At each time t, for each node v_i in state $s_i(t) = 0$, the function f_i outputs $s_i(t+1) = 1$ with probability $p_{e,max}$ if $\eta_1 \ge \eta_{min}$; else f_i outputs $s_i(t+1) = 0$.

The second model, in Figure 1b, the 2mode-threshold model, incorporates the effect of concern for looting, which has been identified as a factor in hurricane evacuation [8]. This model also has an evacuation threshold η_{min} . It is clear from Figure 1 that this model has a smaller range on the x-axis over which the probability of evacuation is non-zero, compared to that of the standard-threshold model. Specifically, families can be concerned that when many of their neighbors have already evacuated, the neighborhood is more vulnerable to looting and crime, and hence do not evacuate. Consequently, when too many families have already evacuated, the looting threshold, denoted by $(\eta_{min} + \eta_c)$, defines the fraction η_1 when a family's p_e drops back to zero. Therefore, at each time t, for each node v_i in state $s_i(t) = 0$, the function f_i outputs $s_i(t+1) = 1$ with

probability $p_{e,max}$ if $\eta_1 \in [\eta_{min}, \eta_{min} + \eta_c]$; else f_i outputs $s_i(t+1) = 0$. This is referred to as the 2mode-threshold model, reflecting the influence of two modes: peer influence to evacuate and looting concern to not evacuate.

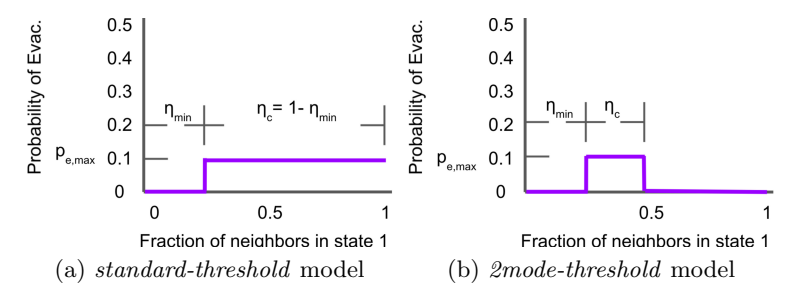


Fig. 1: Agent threshold models. The x-axis (abscissa) is η_1 , the fraction of a node's (agent's) neighbors that are in state 1. The y-axis (ordinate) is p_e , the daily probability that a family evacuates. (a) Classic relative threshold model where the relative threshold η_{min} is the value of η_1 where the daily probability of evacuation becomes non-zero. This is called herein the standard-threshold model. (b) New relative threshold model where there is a concern over looting, where the daily probability of evacuation $p_{e,max}$ returns to zero at $\eta_1 = \eta_{min} + \eta_c$. This is called herein the 2mode-threshold model.

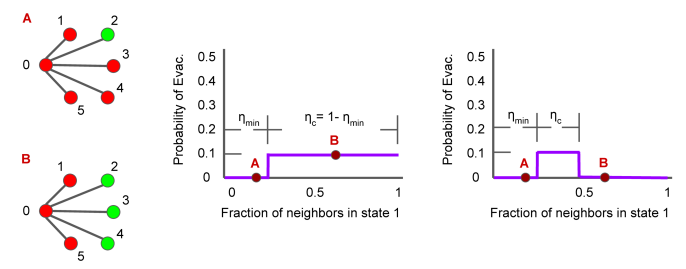


Fig. 2: (Left) Two configurations showing the five neighbors of node 0 that are in state 0 in red and in state 1 in green, labelled A and B. (Center) For the *standard-threshold* model, as η_1 increases, in going from A to B on left, p_e increases from 0 to $p_{e,max}$. (Right) For the *2mode-threshold* model, as η_1 increases, in going from A to B on left, p_e remains at 0; the block wave where $p_e = p_{e,max} > 0$ is missed.

Examples. Figure 2 provides an example of the behavior of the two models for a given ego node $v_0 = 0$ that is in state $s_0(t) = 0$. On the left are two subgraphs labeled A and B. Using the *standard-threshold* model (center graphic), node 0 in subgraph A has $\eta_1 = 1/5$ which is less than $\eta_{min} = 0.25$, and hence $p_e = 0$. That is, $s_0(t+1) = 0$. In subgraph B, however, node 0 has $\eta_1 = 3/5$ which is greater than $\eta_{min} = 0.25$, and hence $p_e = p_{e,max} > 0$. That is, $s_0(t+1) = 1$ with probability $p_{e,max}$. For the 2mode-threshold model (right graphic), node 0 in subgraph A again produces $s_0(t+1) = 0$ for the same reason as for the standard-threshold model. However, for subgraph B, the result for node 0 now changes from that for the standard-threshold model. Node 0 has $s_0(t+1) = 0$

because $\eta_1 > (\eta_c + \eta_{min})$. For this last scenario, the contagion has spread through the network so fast that η_1 has "hopped over" the range $[\eta_{min}, \eta_{min} + \eta_c]$ where $p_e > 0$. This effect will arise in the simulation results.

4 Simulations and Results

4.1 Simulation Description and Parameters

A simulation instance consists of a set of seed nodes that are in state 1 at time t=0. Time progresses forward in integer time steps (each representing one day), and at each time, each node v_i in state $s_i(t)=0$ has its local function f_i executed, in parallel, to determine its next state, i.e., $s_i(t+1)$. If $s_i(t)=1$, then $s_i(t+1)=1$, i.e., a node that reaches state 1 remains in that state. Simulation instances are run in the interval $t \in [0,9]$ to produce $s_i(1)$ through $s_i(10)$ for all $v_i \in V$, $1 \le i \le n$. A simulation consists of a group of simulation instances. Here, we run 100 instances, each instance having a different seed node set; all other inputs are the same across instances. We use as output from the raw simulation results the average and standard deviation of the 100 results at each t. As described in Section 3, each f_i in the computation of $s_i(t+1)$ represents a family behavior such as those in Figure 1. Simulation parameters are given in Table 2.

Table 2: Summary of the parameters and their values used in the simulations.

Parameter	Description			
Network	Miami, FL.			
Number of	Values are 50, 100, 200, 300, 400, and 500 Seed nodes are chosen			
seed nodes, n_s	uniformly at random.			
Threshold model	The standard-threshold (i.e., classic) threshold model of Figure 1a			
	and the 2mode-threshold model of Figure 1b, in Section 3.			
Maximum	The maximum probability of evacuation $p_{e,max}$ of Figure 1. This is			
probability,	a daily probability of evacuation, which is repeated by each family.			
$p_{e,max}$	Discrete values are 0.05 to 0.30 in increments of 0.05.			
Threshold, η_{min}	The minimum value of η_{min} where the probability $p_{e,max}$ becomes			
	greater than zero. Discrete values are 0.01 through 0.09, in increments			
	of 0.01.			
Active threshold	The range in relative degree over which the probabilities $p_e = p_{e,max}$			
range, η_c	are greater than zero. Discrete values are 0.2, 0.4, 0.6, 0.8, 0.90, and			
	0.95. Values of $\eta_c = 1 - \eta_{min}$ represent the standard-threshold model,			
	whereas lesser values represent the 2mode-threshold model.			

4.2 Simulation Results

Comparison of the 2mode-threshold and standard-threshold Models Basic simulation results in this section are provided for the 2mode-threshold model. Figure 3a shows the fraction of families newly evacuating on each of the ten days leading up to hurricane arrival, for numbers n_s of seed nodes up to 500 families. Inputs for the 2mode-threshold model are $\eta_{min} = 0.05$, $\eta_c = 0.2$, and $p_{e,max} = 0.3$. The fraction of evacuating families is initially small, growing

noticeably over the last four days. Error bars denoting \pm one standard deviation indicate that the scatter across the 100 simulation instances is relatively small. Figures 3b and 3c show cumulative fraction of evacuating families for the 2mode-threshold and standard-threshold models, respectively. The former plot plateaus for greater numbers of seed nodes, reflecting the looting threshold effect, while the latter plot shows no such constraint.

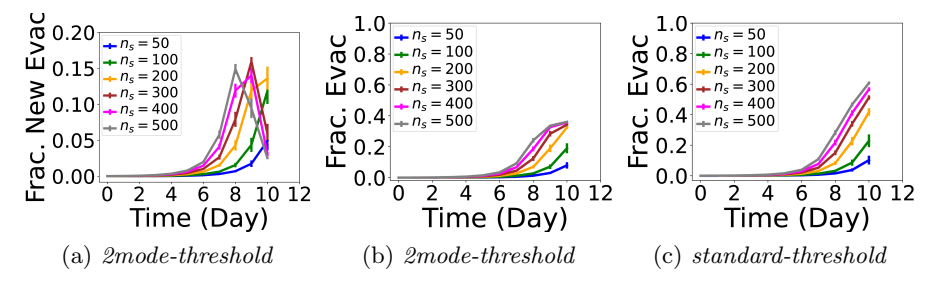


Fig. 3: Simulation results of the fraction of evacuating families in Miami, FL versus time. Fractions of (a) newly evacuating families and (b) cumulative evacuating families as a function of time for the 2mode-threshold model. Model conditions are $\eta_c = 0.2$, $\eta_{min} = 0.05$, and $p_{e,max} = 0.30$. (c) Fraction of cumulative evacuating families for the standard-threshold model, with the same properties, except that $\eta_c = 1 - \eta_{min} = 0.95$. All data points on all plots display \pm one standard deviation; the variability over 100 simulation instances is not large.

Effect of Evacuation Threshold η_{min} Figure 4 shows the effect of η_{min} for the 2mode-threshold model for three values of $p_{e,max}$. Figures 4b and 4c show that there is a precipitous dropoff in evacuation fraction over a narrow range in η_{min} , indicative of a phase transition. These plots demonstrate that this phenomenon is persistent across different values of $p_{e,max}$ and n_s .

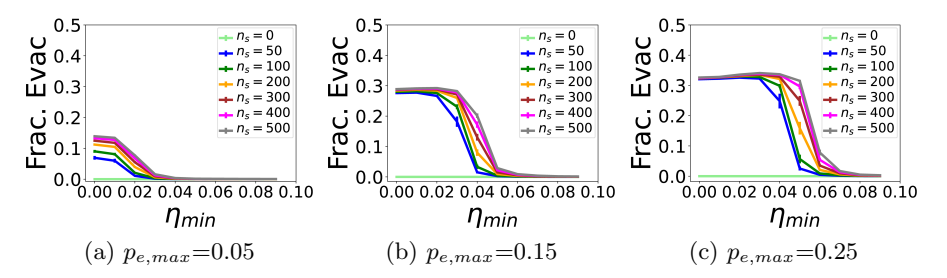


Fig. 4: Effect on cumulative evacuation fraction of η_{min} for the 2mode-threshold model at day t=10. Here, $\eta_c=0.2$ and $p_{e,max}$ is (a) 0.05 (b) 0.15, and (c) 0.25. For larger $p_{e,max}$, the evacuation fraction changes markedly over a small range in η_{min} , suggesting a phase transformation. All data points on all plots display one standard deviation error bars; the variability over 100 simulation instances is not large.

Effect of Range η_c Over Which $p_{e,max} > 0$ Figure 5 shows the effect of η_c on evacuation fraction (at day 10). The left-most plot is the largest fraction of

newly evacuating families on any day; the remaining two plots are cumulative fractions of evacuating families. Most curves in Figure 5a are flat for $\eta_c > 0.4$, indicating a saturation in behavior at larger η_c . This effect is also observed in Figure 5c, for a greater value of η_{min} . Even in the middle plot, the curves saturate at lesser η_c for $p_{e,max} \leq 0.10$, but exhibit more changes in evacuation fraction with η_c for $p_{e,max} > 0.1$. The point is that the two models—2mode-threshold and standard-threshold models—have as their primary difference the values of η_c . These results demonstrate that behavior of the 2mode-threshold model can be the same as that of the standard-threshold model for values of η_c that are far less than $\eta_c = 1 - \eta_{min}$, as is the case for the standard-threshold model. This effect is not observed over all conditions, but nonetheless over a significant range of conditions.

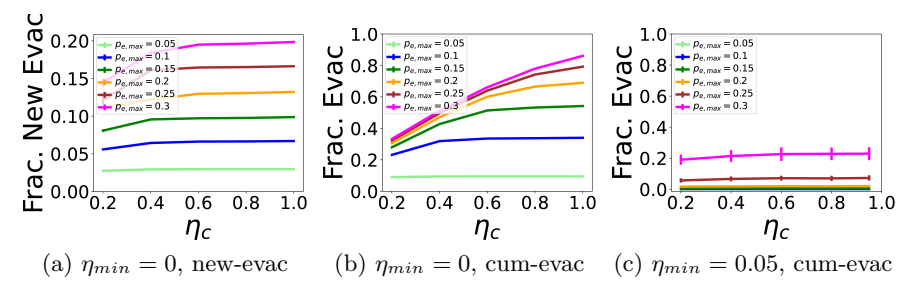


Fig. 5: Effect of η_c on the 2mode-threshold model predictions of evacuation rates in Miami, FL. Each data point is over the 10 days leading up to hurricane landfall. Here, $n_s=100$ families and $p_{e,max}$ is given in legends. (a) Maximum fractions of new evacuations on any day for $\eta_{min}=0$. (b) Cumulative evacuation curves for $\eta_{min}=0$. (c) Cumulative evacuation curves for $\eta_{min}=0.05$. All data points on all plots display \pm one standard deviation.

Combined Effect of Evacuation Threshold η_{min} and Maximum Probability $p_{e,max}$ Figure 6 shows the combined effect of variations in η_{min} and $p_{e,max}$ on evacuation fraction. The effect is somewhat surprising in that it can be considered counterintuitive. Figures 6a and 6b depict, respectively, the largest fraction of newly evacuating nodes, on any day $t \in [1, 10]$, and the cumulative evacuation fraction. Both plots show curves that are not non-increasing, which is at first counterintuitive. The curve $p_{e,max} = 0.3$ in Figure 6b, for example, shows a discernible increasing trend in evacuation fraction as η_{min} increases in the range [0.01, 0.05]. One would suspect that these curves would be non-increasing as in Figures 4a and 4b because increasing η_{min} means that a node v_i in state 0 with small fractions of neighbors in state 1 would not produce $p_e = p_{e,max} > 0$ (i.e., a non-zero probability of evacuation).

The reason for this behavior is as follows. Data (not provided here for space reasons) demonstrate that the speed of contagion spread increases with $p_{e,max}$. Thus, for a node v_i in state 0, increasing $p_{e,max}$ causes more neighbors of v_i to change to state 1 earlier, in a sense "flooding" the neighborhood of v_i . This means that it is advantageous to increase η_{min} so that the block wave in Figure 1b gets moved to the right so that $p = p_{e,max} > 0$ is operative for greater η_1 . If

the block wave does not move further to the right, then the behavior at the right in Figure 2, point labeled B, will be operative and the contagion will not propagate. This reasoning suggests that the effect will become more pronounced with increasing $p_{e,max}$, which is what Figure 6b shows.

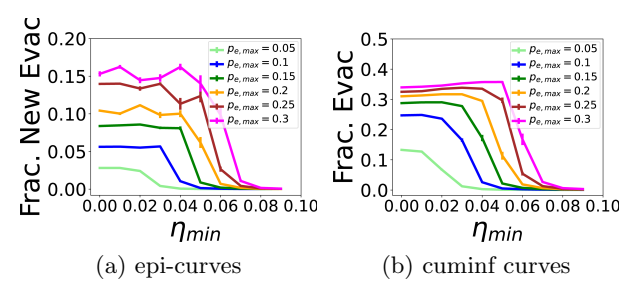


Fig. 6: Simulation results for Miami, FL. The plots are for the 2mode-threshold model where $\eta_c = 0.2$, and η_{min} and $p_{e,max}$ vary per the plots. The number of seed nodes is 400 families. The y-axes are: (a) largest fraction of families evacuating on any day $t \in [1, 10]$, and (b) cumulative fraction of families evacuating. These plots show counterintuitive results as described in the text.

Spatial Aspects of Evacuation Figure 7 contains heat maps of evacuation probabilities for the high population density region of Miami, FL. The maps are generated as follows. Each family dwelling is geo-located. The high population density region of the city of Miami is gridded into 156 cells in the horizontal and 137 cells in the vertical directions, producing 21372 rectangular cells. For each of the families v_i within a cell, the fraction ρ_i of the 100 simulation instances in which the family evacuates is computed. The average value for a cell j, $\rho_{cell,j}$, which is plotted, is the average value of all ρ_i whose homes are in cell j. Results at t=10 days are provided for both models. Although there are differences among cells, the results indicate that at a high level, the evacuation rates across the high population density region of Miami are fairly uniform. Evacuation rates are greater for the standard-threshold model.

Policy implication and causal explanation First, a sensible model at an individual level (e.g., Figure 1) may give rise to counterintuitive behavior such as that shown in Figure 6. This is a well-know signature of "complex systems." Second, from a practical standpoint, the takeaway is that it is important to minimize η_{min} and to maximize $\eta_{min} + \eta_c$ in order to keep $p_{e,max}$ operative over the greatest range of η_1 . This takeaway is consistent with the statement: to increase the evacuation, allay families' concerns over looting. From a modeling perspective, this means that interventions should seek to make families' behaviors more like that in Figure 1a, and less like that in Figure 1b. And while this might seem obvious from an intuitive viewpoint, the contribution here is that this analysis provides a causal explanation. Third, the results of this paper suggest the following: government-based interventions to allay people's concerns about looting (e.g., via increased patrols)—to increase η_c —and to incentivize evacuation—to

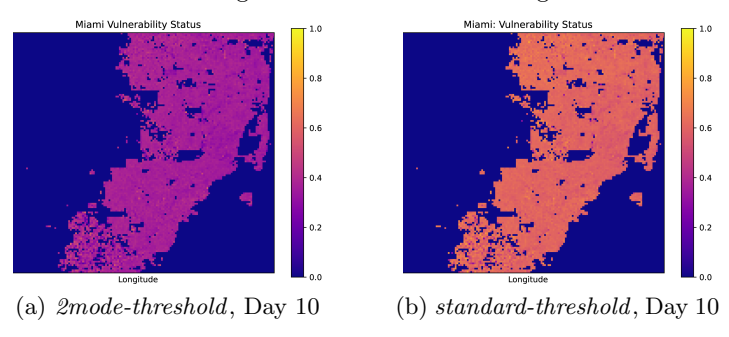


Fig. 7: Heat maps of the high population density region of Miami, representing the average evacuation rates of all families within each gridcell. There are 156×137 cells in the horizontal and vertical directions. In these plots, $\eta_{min} = 0.05$, $p_{e.max} = 0.3$, $n_s = 500$, and $\eta_c = 0.2$ and $1 - \eta_{min}$, respectively.

increase $p_{e,max}$. Looting and rioting experiences from Hurricane Katrina caused police to warn against human-inflicted damage in future hurricanes [7]. This work suggested that these warnings may also encourage greater evacuation.

5 CONCLUSIONS

We present the first study of evacuation dynamics in a large urban region. Using an agent-based model, we find that peer influence and looting concerns have a significant impact on the fraction of people who evacuate. We observe the evacuation dynamics are quite sensitive to the thresholds and probability of evacuation. Our work highlights the importance of modeling detailed representations of the social network, the geospatial attributes of home locations, and realistic peer behaviors, in understanding policies and response to natural disasters. A shortcoming of our work is that we only address human contact networks; we do not include the effects of social media. We speculate that social media will not change the overall trends since the looting effect will persist. Future work includes tailoring the curves of the models in Figure 1 for families based on household demographics. Our current plan is to make the model available in a future release of a simulation system [11] within a cyberinfrastructure [1].

Acknowledgment. We thank the anonymous reviewers for their helpful feedback. We thank our colleagues at NSSAC and Research Computing at the University of Virginia. This work has been partially supported by University of Virginia Strategic Investment Fund award number SIF160, NSF Grant OAC-1916805 (CINES), NSF CRISP 2.0 (CMMI Grant 1916670 and CMMI Grant 1832693), NSF CMMI-1745207 and NSF Award 122135.

References

1. Ahmed, N.K., Alo, R.A., et al.: net.science: A cyberinfrastructure for sustained innovation in network science and engineering. In: Proceedings of the Gateways

- 2020 Conference (Science Gateways Community Institute) (2020)
- Barrett, C.L., Beckman, R.J., et al.: Generation and analysis of large synthetic social contact networks. In: Winter Simulation Conference (WSC). pp. 1003–1014 (2009)
- 3. Burnside, R.: Leaving the Big Easy: An examination of the hurricane evacuation behavior of New Orleans residents before Hurricane Katrina. Journal of Public Management and Social Policy 12, 49–61 (01 2006)
- 4. Centola, D., Macy, M.: Complex contagions and the weakness of long ties. American Journal of Sociology 113(3), 702–734 (2007)
- Chen, J., Hoops, S., et al.: Prioritizing allocation of covid-19 vaccines based on social contacts increases vaccination effectiveness. medRxiv (2021), https://www. medrxiv.org/content/early/2021/02/06/2021.02.04.21251012
- 6. Cole, T.W., Fellows, K.L.: Risk communication failure: A case study of new orleans and Hurricane Katrina. Southern Communication Journal 73(3), 211–228 (2008)
- 7. Faucon, C.: The suspension theory: Hurricane katrina looting, property rights, and personhood. Louisiana Law Review 70(4), 1303–1338 (2010)
- 8. Halim, N., Jiang, F., Khan, M., Meng, S., Mozumder, P.: Household evacuation planning and preparation for future hurricanes: Role of utility service disruptions. Transportation Research Record (2021)
- 9. Halim, N., Kuhlman, C.J., Marathe, A., Mozumder, P., Vullikanti, A.: Two-mode threshold graph dynamical systems for modeling evacuation decision-making during disaster events. In: Complex Networks. pp. 519–531 (2019)
- Kempe, D., Kleinberg, J., Tardos, E.: Maximizing the spread of influence through a social network. In: Proc. ACM KDD. pp. 137–146 (2003)
- 11. Kishore, A., Machi, L., et al.: A framework for simulating multiple contagions over multiple networks. In: Complex Networks (2021)
- 12. Kuhlman, C., Marathe, A., Vullikanti, A., Halim, N., Mozumder, P.: Increasing evacuation during disaster events. In: Autonomous Agents and Multiagent Systems (AAMAS). pp. 654–662 (2020)
- 13. Masters, J.: A look back at the horrific 2020 atlantic hurricane season; Yale Climate Connections. https://yaleclimateconnections.org/2020/12/a-look-back-at-the-horrific-2020-atlantic-hurricane-center/, accessed: 2020-08-13
- 14. Riad, J.K., Norris, F.H., Ruback, R.B.: Predicting evacuation in two major disasters: Risk perception, social influence, and access to resources1. Journal of Applied Social Psychology 29(5), 918–934 (1999)
- 15. Shultz, J.M., Galea, S.: Mitigating the Mental and Physical Health Consequences of Hurricane Harvey. JAMA 318(15), 1437–1438 (10 2017)
- 16. Smith, A.: 2020 U.S. billion-dollar weather and climate disasters in historical context. https://www.climate.gov/news-features/blogs/beyond-data/2020-us-billion-dollar-weather-and-climate-disasters-historical (Aug 20, 2021)
- 17. Wong, S., Shaheen, S., Walker, J.: Understanding evacuee behavior: A case study of hurricane irma. https://escholarship.org/uc/item/9370z127
- Yin, W., Murray-Tuite, P., Ukkusuri, S.V., Gladwin, H.: An agent-based modeling system for travel demand simulation for hurricane evacuation. Transportation Research Part C: Emerging Technologies 42, 44–59 (2014)
- 19. Zhu, Y., Xie, K., Ozbay, K., Yang, H.: Hurricane evacuation modeling using behavior models and scenario-driven agent-based simulations. Procedia Computer Science 130, 836–843 (2018)